

Modeling Nanowire and Double-Gate Junctionless Field-Effect Transistors

Being the first book on the topic, this is a comprehensive introduction to the modeling and design of junctionless field-effect transistors. Beginning with a discussion of the advantages and limitations of the technology, the authors provide a thorough overview of published analytical models for double-gate and nanowire configurations, before offering a general introduction to the EPFL charge-based model of junctionless FETs. Important features are introduced gradually, including nanowire versus double-gate equivalence, technological design space, junctionless FET performances, short-channel effects, transcapacitances, asymmetric operation, thermal noise, interface traps, and the junction FET. Additional features compatible with biosensor applications are also discussed. This is a valuable resource for students and researchers looking to understand more about this new and fast-developing field.

Farzan Jazaeri is a Scientist at the École Polytechnique Fédérale de Lausanne where his research interests focus on semiconductor devices and physics, and particularly on the modeling and fabrication of field-effect transistors.

Jean-Michel Sallese is a Senior Scientist at the École Polytechnique Fédérale de Lausanne. He specializes in the analytical modeling of bulk and multigate field-effect transistors.

Modeling Nanowire and Double-Gate Junctionless Field-Effect Transistors

FARZAN JAZAERI

École Polytechnique Fédérale de Lausanne

JEAN-MICHEL SALLESE

École Polytechnique Fédérale de Lausanne



CAMBRIDGE
UNIVERSITY PRESS

Cambridge University Press
978-1-107-16204-4 — Modeling Nanowire and Double-Gate Junctionless Field-Effect Transistors
Farzan Jazaeri, Jean-Michel Sallese
Frontmatter
[More Information](#)

CAMBRIDGE UNIVERSITY PRESS

University Printing House, Cambridge CB2 8BS, United Kingdom
One Liberty Plaza, 20th Floor, New York, NY 10006, USA
477 Williamstown Road, Port Melbourne, VIC 3207, Australia
314–321, 3rd Floor, Plot 3, Splendor Forum, Jasola District Centre, New Delhi – 110025, India
79 Anson Road, #06-04/06, Singapore 079906

Cambridge University Press is part of the University of Cambridge.

It furthers the University's mission by disseminating knowledge in the pursuit of education, learning, and research at the highest international levels of excellence.

www.cambridge.org
Information on this title: www.cambridge.org/9781107162044
DOI: 10.1017/9781316676899

© Cambridge University Press 2018

This publication is in copyright. Subject to statutory exception and to the provisions of relevant collective licensing agreements, no reproduction of any part may take place without the written permission of Cambridge University Press.

First published 2018

Printed in the United Kingdom by Clays, St Ives plc

A catalogue record for this publication is available from the British Library.

ISBN 978-1-107-16204-4 Hardback

Cambridge University Press has no responsibility for the persistence or accuracy of URLs for external or third-party internet websites referred to in this publication and does not guarantee that any content on such websites is, or will remain, accurate or appropriate.

Contents

	<i>Foreword</i>	<i>page xi</i>
	<i>Preface</i>	xiii
	<i>List of Abbreviations</i>	xv
	<i>List of Symbols</i>	xvii
1	Introduction	1
	1.1 The Birth of the Transistor	1
	1.2 The Metal-Oxide–Semiconductor Field-Effect Transistor	1
	1.3 Moore’s Law, Limits of CMOS Scaling, and Alternative MOSFET Structures	2
	1.3.1 Scaling in Bulk MOSFETs	2
	1.3.2 Silicon-on-Insulator MOSFETs	3
	1.4 The Junctionless Concept	4
	1.4.1 Working Principle of Junctionless MOSFETs	4
	1.4.2 Diversity in Junctionless Architectures	6
	1.5 Short-Channel Effects in Junctionless FETs	9
	1.6 Mobility in Junctionless FETs	10
	1.7 The Critical Aspect of Random Dopant Fluctuation	11
	1.7.1 Random Dopant Fluctuations in Junctionless FETs	12
	1.8 Summary	14
2	Review on Modeling Junctionless FETs	15
	2.1 Modeling Junctionless Double-Gate MOSFETs	15
	2.1.1 Full Depletion Approximation	15
	2.1.2 Enhanced Depletion Approximation	17
	2.1.3 Surface Potential-based Approach	17
	2.1.4 Simplified Current Model Involving Pinch-Off	19
	2.1.5 Semiempirical Charge-based Approach	20
	2.1.6 Analytical Approach based on Conventional Inversion-Mode MOSFETs	20
	2.1.7 Parabolic Approximation and Full-Range Drain Current	20
	2.1.8 Gaussian Distribution of Mobile Charge Density	21
	2.1.9 Simple Model to Estimate Junctionless FET Performances	22

vi	Contents	
	2.1.10 Explicit Drain Current Model Relying on Charge-based Approach	23
	2.1.11 Modeling of Quantum Mechanical Effects	23
	2.1.12 Short-Channel Effects in Subthreshold	24
	2.1.13 Transcapacitance Modeling	25
	2.1.14 Modeling Asymmetry in Junctionless Double-Gate MOSFETs	25
	2.2 Modeling Junctionless Nanowire MOSFETs	25
	2.2.1 Short-Channel Effects in the Subthreshold	27
	2.2.2 Transcapacitance Modeling in Junctionless Nanowire FETs	27
	2.2.3 Quantum Mechanical Effects in Junctionless Nanowire FETs	28
	2.3 Summary	28
3	The EPFL Charge-based Model of Junctionless Field-Effect Transistors	29
	3.1 Charge-based Modeling of Junctionless Double-Gate Field-Effect Transistors	29
	3.1.1 Recalling Basics of Semiconductor Statistics	29
	3.1.2 Approximate Solution of the Poisson–Boltzmann Equation in Junctionless Double-Gate MOSFET	32
	3.1.3 Introduction of Symmetric Gate Capacitances	35
	3.1.4 Derivation of Explicit Voltage–Charge Relationships	36
	3.1.5 Analytical versus Numerical Simulations	38
	3.1.6 Threshold Voltage in Junctionless FETs	41
	3.1.7 Derivation of the Channel Current	41
	3.1.8 Evaluation of the Charge Integral	44
	3.1.9 General Treatment of the Current in Junctionless Double-Gate MOSFETs	45
	3.1.10 Simulation Results	46
	3.2 A Common Core Model for Junctionless Nanowires and Symmetric DG FETs	50
	3.2.1 Analysis of Electrostatics in Junctionless Nanowire FETs	50
	3.2.2 Derivation of the Current in a Junctionless Nanowire	53
	3.2.3 Simulations	53
	3.3 Explicit Model for Long-Channel Gate-All-Around Junctionless MOSFETs	55
	3.3.1 Approximated Solution in Depletion	57
	3.3.2 Approximated Solution in Accumulation Mode	58
	3.3.3 Approximated Solution in Weak Accumulation Mode	58
	3.4 Summary	58
4	Model-Driven Design-Space of Junctionless FETs	60
	4.1 <i>Off</i> -Current and Inversion Layer in Junctionless FETs	60
	4.2 Electrostatics in Junctionless Double-Gate MOSFET including Minority Carriers	61

	Contents	vii
	4.2.1 Role of the Channel Potential	64
	4.2.2 Estimation of the Critical Potentials	65
	4.2.3 Minimum Mobile Charge Density	69
	4.2.4 Estimation of <i>On/Off</i> -Current Ratio in Long-Channel Junctionless FETs	69
	4.2.5 Rail-to-Rail Supply Voltage Benchmark	73
	4.3 Summary	75
5	Generalization of the Charge-based Model: Accounting for Inversion Layers	76
	5.1 Electrostatics including Minority Carriers	76
	5.1.1 Coexistence of Depletion and Inversion: General Treatment	78
	5.1.2 Charge–Voltage Relationships	80
	5.1.3 Inversion Layer-Induced Capacitance in Junctionless Double-Gate MOSFET	81
	5.2 Simulations and Model Assessments	82
	5.2.1 Impact of Hole Layer on Drain Current	83
	5.3 Summary	85
6	Predicted Performances of Junctionless FETs	86
	6.1 Device Scaling Principle	86
	6.2 Considerations on Intrinsic-Delay Scaling	88
	6.3 Summary	91
7	Short-Channel Effects in Symmetric Junctionless Double-Gate FETs	92
	7.1 Electrostatics in Short-Channel Junctionless DG MOSFETs in the Subthreshold	92
	7.1.1 Approximate Solution of the Potential Distribution	93
	7.1.2 Assessment of the Center Potential with Regard to Numerical Simulations	94
	7.2 Subthreshold Current, Subthreshold Swing, and DIBL	98
	7.2.1 The Minimum Potential	98
	7.2.2 Channel Current in Subthreshold	100
	7.2.3 Subthreshold Swing in Junctionless FETs	103
	7.2.4 DIBL in Junctionless FETs	104
	7.3 Summary	107
8	Modeling AC Operation in Symmetric Double-Gate and Nanowire JL FETs	108
	8.1 Transcapacitance Matrix in Symmetric Double-Gate FETs	108
	8.2 General Case	110
	8.2.1 Expressing dy versus dV_{ch}	111
	8.2.2 Expressing $Q_m(y)dV_{ch}$	112
	8.2.3 Expressing y/L_G versus $Q_m(y)$	112

8.3	Special Case of a Channel Uniformly Depleted/Accumulated	116
8.3.1	Channel in Depletion Mode	116
8.3.2	Channel in Accumulation Mode	118
8.4	Analytical Expressions for the Local Charge Derivatives	119
8.5	Simulations and Discussion	121
8.6	Cubic Approximation of $Q_m(y)$ and Transcapacitances	124
8.6.1	Hybrid Channel	124
8.6.2	Uniform Channels	126
8.6.3	Evaluation of Flat-Band Position along the Hybrid Channel	127
8.6.4	Evaluation of the Transcapacitances	127
8.7	Transcapacitances in Gate-All-Around Junctionless Nanowire FETs	130
8.7.1	Equivalent Parameters Definition	130
8.7.2	Simulations	131
8.8	A Simplified Approach to Transcapacitance Modeling in Junctionless Nanowire FETs	132
8.8.1	Channel in Depletion Mode	133
8.8.2	Channel in Accumulation Mode	135
8.9	Summary	138
9	Modeling Asymmetric Operation of Double-Gate Junctionless FETs	139
9.1	General Considerations in Asymmetric Junctionless Double-Gate FETs	139
9.2	Analysis Restricted to Depletion or Accumulation	142
9.2.1	Potential Extremum Inside the Channel	142
9.2.2	Extremum Potential Outside the Channel	145
9.2.3	The Iterative Solution	146
9.2.4	Simulations	146
9.3	Coexistence of Depletion and Accumulation	148
9.3.1	Modeling Depleted–Accumulated Channels	148
9.3.2	Simplifying Assumptions	149
9.3.3	Assessment of Continuity at the Transition Coordinates	149
9.4	Derivation of the Current	150
9.5	Simulations	151
9.5.1	Potential Induced Asymmetry	151
9.5.2	Structural Asymmetry	151
9.5.3	Approximate Expression for the Current	151
9.5.4	Limitations	153
9.6	Summary	153
10	Modeling Noise Behavior in Junctionless FETs	155
10.1	Thermal-Noise Modeling	155
10.2	Induced Gate Noise in Junctionless FET	159
10.3	Cross-Correlation Noise in Junctionless FETs	161
10.4	Summary	163

	Contents	ix
11	Carrier Mobility Extraction Methodology in JL and Inversion-Mode FETs	164
11.1	Y Function and Mobility Extraction in Junctionless FETs	164
11.2	Model-Independent Mobility-Extraction Method in Junctionless FETs	166
11.2.1	General Treatment	166
11.2.2	Mobility Extraction in Double-Gate Junctionless FETs	169
11.2.3	A Simplified Approach	170
11.3	Extending the Method to Inversion-Mode FETs	171
11.4	Limitations	172
11.5	Summary	173
12	Revisiting the Junction FET: A Junctionless FET with an ∞ Gate Capacitance	174
12.1	Principle Operation of the JFET	174
12.2	Charge-based Modeling of Double-Gate JFETs	175
12.2.1	Charge–Voltage and Pinch-Off Voltage in Double-Gate JFETs	175
12.2.2	Channel Current in Double-Gate JFETs	176
12.2.3	Simulations	177
12.3	Modeling Small Signals in JFETs	177
12.3.1	Transconductance	177
12.3.2	Transcapacitances in JFET	179
12.3.3	Simulations	181
12.4	Summary	182
13	Modeling Junctionless FET with Interface Traps Targeting Biosensor Applications	183
13.1	Principle of Semiconductor-based Field-Effect Biosensors	183
13.2	Modeling Surface Traps in Junctionless FETs	185
13.2.1	General Considerations for Interface Traps	185
13.2.2	Modeling Trapped Charges at the Semiconductor/Insulator Interface in Junctionless FETs	186
13.2.3	Current Derivation	192
13.2.4	The Case of Continuous Energy-Trap Distribution	193
13.2.5	Summary	195
Appendix A	Design-Space of Twin-Gate Junctionless Vertical Slit FETs	197
A.1	Design-Space of Twin-Gate Junctionless Vertical Slit FETs	197
A.1.1	Device Structure	197
A.1.2	Electrostatics in Junctionless VeSFET and Design-Space	197
Appendix B	Transient <i>Off</i>-Current in Junctionless FETs	200
Appendix C	Derivatives of Mobile Charge Density with Respect to V_{GS} and V_{DS}	203
Appendix D	Global Charge Density at Drain in Depletion Mode	204

x **Contents**

Appendix E Global Charge Density at Drain in Accumulation Mode	206
Appendix F The EPFL Junctionless MODEL	208
F.1 The EPFL-Junctionless Model Modules	208
F.2 Source Code Modules and Library	209
F.3 DC Implementation in Junctionless FETs	210
F.4 AC Implementation in Junctionless FETs	211
F.5 Junctionless Double-Gate and Nanowire FET Amplifier	213
F.6 Junctionless Double-Gate and Nanowire FET Inverter	214
 <i>References</i>	215
<i>Index</i>	231

Foreword

Since its first publication in 2009, the junctionless transistor [1] proved to be a very popular device amongst semiconductor research groups worldwide. Junctionless transistors are very simple to manufacture and the junctionless architecture has been successfully applied to many semiconductor materials including single-crystal and polycrystalline silicon and germanium, III-V compounds, ZnO, Indium-tin oxide (ITO), transition metal dichalcogenides, etc.

Figure 0.1 shows the number of publications and citations in Web of Knowledge corresponding to the search word “junctionless transistor”. Well over a hundred papers were published on junctionless transistors each year during 2009–16, with more than a thousand corresponding citations.

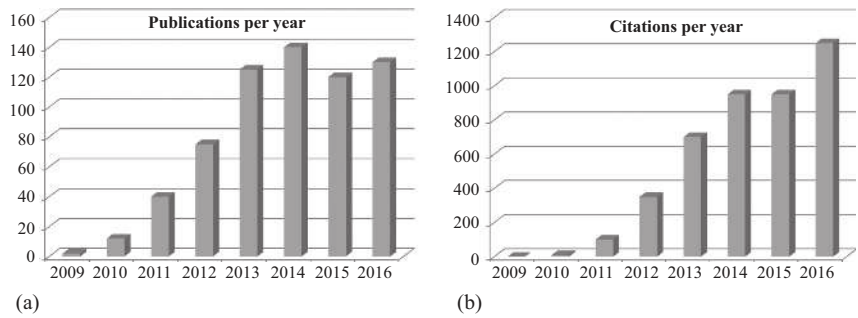


Figure 0.1 The number of publications (a) and citations (b) per year, corresponding to the search word “junctionless transistor” in Web of Knowledge.

Junctionless transistors are also increasingly being used as detectors such as gas, chemical, biochemical, and pH sensors [2, 3]. They are also being considered for the formation of low-thermal-budget active interconnects in future monolithic 3D integrated circuits [4].

Although the electrical characteristics of a junctionless transistor are quite similar to those of a conventional inversion-mode device, there are key differences in transport and capacitance properties: transport in a junctionless transistor is largely in the bulk of the semiconductor instead of in an inversion channel. As a result, surface scattering and trapping of carriers is reduced, which improves noise figure and allows one to make transistors in materials that have problematic interface properties, *n*-channel germanium MOSFETs being a good example.

Accurate modeling of the junctionless transistor is essential for comparing the performance of these devices with those of other types of transistors and for different types of applications. The publication of the book *Modeling Nanowire and Double-Gate Junctionless Field-Effect Transistors* by Doctors Farzan Jazaeri and Jean-Michel Sallese, two renown experts in the field, is thus timely and will bring valuable information to those interested in advanced device physics, simulation, and design.

Jean-Pierre Colinge
CEA-LETI, France

Preface

Metal-oxide semiconductor field-effect transistor scaling is following the prediction of the Moore's law enunciated in 1965 [5]. So far, this trend for miniaturization has never been invalidated, enabling the industry of semiconductors to cope with the everlasting demand for higher performance at lower cost. However, this scaling becomes increasingly difficult to follow due to inherent process and device performance limitations for technology nodes beyond tens of nm. To stand the pace of downscaling, nonclassical device architectures have been continuously proposed in the ITRS roadmap.

The junctionless field-effect transistor is one of these nanoelectronics devices that is expected to withstand the downscaling of Complementary Metal-Oxide-Semiconductor (CMOS) technology by enabling easier fabrication processes, while allowing high performance. In addition, semiconductor nanowires largely used for label-free biosensing are essentially junctionless FETs without any gate.

Therefore, since the first implementation of junctionless FET nanowires by J. P. Colinge in 2009, growing interest in these devices in different fields of research motivated the authors to write a book dedicated to analytical modeling of double-gate and nanowire junctionless FETs. In contrast to the abundant literature on modeling and compact modeling of inversion-mode MOSFETs, analytical modeling of field-effect transistors without junctions is still following different strategies.

After discussing the advantages and limitations of junctionless field-effect transistors in the first introductory chapter, a thorough overview of published analytical models for double-gate and nanowires configurations is presented in Chapter 2, including the mains assumptions which are introduced.

In Chapter 3 and beyond, the analytical model of the so-called EPFL junctionless field-effect transistor is presented. After discussing the roots ending with a charge-based model valid in all the regions of operation, important features are introduced gradually in Chapters 4–13, each of which targets a specific feature. These topics include nanowire versus double-gate equivalence, technological design-space, junctionless FET performance, short-channel effects, transcapacitances, asymmetric operation, thermal noise, interface traps, and a revisited model for JFETs. In addition a general mobility extraction technique is proposed.

We suggest readers see Chapter 3 for a general introduction to the charge-based model before proceeding further. This is where the main ideas are introduced that will thus be used in the following chapters.

We hope this book will be useful to people interested in modeling these new types of field-effect transistors, which are likely to find diverse applications, not only in nanoelectronics, but also in a large variety of biosensors.

The authors would like to acknowledge Doctors Lucian Barbut and Didier Bouvet who actively participated in the research done at EPFL and also Doctors Maria-Anna Chalkiadaki, Wladek Grabinski, and Professor Christian Enz who provided invaluable support. Many thanks to Professors Christophe Lallement, Benjamin Iñiguez, Matthias Bucher and Ashkhen Yesayan for their involvement in this research. Finally, we would like to thank warmly Dr. Adil Koukab, Dr. Anurag Mangla, and Nikolaos Makris for the very constructive scientific discussions.

We are also very grateful to Elizabeth Horne, Heather Brolly, and Abirami Ulaganathan who continuously assisted us in the preparation of the book.

Last, we would like to warmly thank our families and our parents. Thanks in particular to Ferdos, Jamal, Farshid, Farzad, and Parnian and Baya, Yoanna, Marion, and Loris for their support and understanding during this seemingly endless task.

Farzan Jazaeri and Jean-Michel Sallese

Abbreviations

Abbreviation	Expansion
AC	Alternating current
Acc	Accumulation
ADS	Advanced design system
AM	Accumulation-mode
ASIC	Application specific integrated circuit
ASD	Asymmetric double-gate
BJT	Bipolar junction transistor
BOX	Buried oxide
CMOS	Complementary metal-oxide-semiconductor
DC	Direct current
Dep	Depletion
DFT	Density functional theory
DG	Double-gate
DIBL	Drain-induced barrier lowering
EDL	Electrical double layer
FB	Flat-band
FET	Field-effect transistor
FinFET	Fin-based field-effect transistor
GAA	Gate-all-around
GCA	Gradual-channel approximation
GIDL	Gate-induced drain leakage
Hyb	Hybrid
IC	Integrated circuits
IGFET	Insulated-gate semiconductor field-effect transistor
IGN	Induced-gate noise
IM	Inversion-mode
ISFET	Ion-sensitive field-effect transistor
ITRS	International technology roadmap for semiconductors
JFET	Junction FET
JL	Junctionless
LHS	Left-hand side
MOSFET	Metal-oxide semiconductor field-effect transistor
NEGF	Non-equilibrium green's function
NW FET	Nanowire field-effect transistor

Abbreviation	Expansion
PSD	Power spectral density
QCE	Quantum confinement effect
QEB	Quantum energy balance
QHO	Quantum harmonic oscillator
QME	Quantum mechanical effect
QW	Quantum well
RHS	Right-hand side
RF	Radio frequency
RSCE	Reverse short-channel effect
SC	Semiconductor channel
SCE	Short-channel effect
SOI	Silicon-on-insulator
SS	subthreshold swing
SW	Switch
TCAD	Technology computer-aided design
VeSFET	Vertical slit semiconductor field-effect transistor
VeSTIC	Integrated circuit vesfet-based

Symbols

Symbol	Description	Unit
q	Electron charge	<i>Coulomb</i>
T	Absolute temperature	Kelvin
h	Planck's constant	<i>J.s</i>
$\hbar = h/(2\pi)$	Reduced Planck's constant	<i>J.s</i>
k_B	Boltzmann's constant	<i>J/K</i>
ϵ_0	Permittivity of free space	<i>F/m</i>
ϵ_{si}	Permittivity of silicon	<i>F/m</i>
ϵ_{ox}	Permittivity of SiO ₂	<i>F/m</i>
m_e^*	Electron effective mass	<i>Kg</i>
m_h^*	Hole effective mass	<i>Kg</i>
N_c	Effective density of states in conduction band	m^{-3}
N_v	Effective density of states in valence band	m^{-3}
$g_c(E)$	Density of states in conduction band	$m^{-3} J^{-1}$
$g_v(E)$	Density of states in valence band	$m^{-3} J^{-1}$
n_i	Intrinsic carrier concentration	m^{-3}
E_g	Silicon band-gap	<i>eV</i>
E_i	Intrinsic Fermi energy	<i>eV</i>
E_f	Fermi energy	<i>eV</i>
E_c	Bottom of conduction band energy level	<i>eV</i>
E_{cM}	Top of conduction band energy level	<i>eV</i>
E_{vm}	Bottom of valence band energy level	<i>eV</i>
E_v	Top of valence band energy level	<i>eV</i>
σ_n	Cross section of electrons	m^2
σ_p	Cross section of holes	m^2
e_n	Electron emission coefficient	s^{-1}
e_p	Hole emission coefficient	s^{-1}
v_n	Electron average velocity	ms^{-1}
v_p	Hole average velocity	ms^{-1}
τ_c	Average scattering time	<i>s</i>
σ	Average conductivity	$\Omega^{-1}m^{-1}$
$J_{n,drift} = qn\mu_n$	Drift electron current density	Acm^{-2}
$J_{p,drift} = qp\mu_p$	Drift hole current density	Acm^{-2}
$J_{n,diffusion}$	Diffusion electron current density	Acm^{-2}
$J_{p,diffusion}$	Diffusion hole current density	Acm^{-2}
J_{drift}	Total drift current density	Acm^{-2}
$J_{diffusion}$	Total diffusion current density	Acm^{-2}

Symbol	Description	Unit
$f(E)$	Fermi–Dirac statistic	–
$D_n = \mu_n k_B T$	Electron diffusion constant (Einstein relation)	$m^2 s^{-1}$
$D_p = \mu_p k_B T$	Hole diffusion constant (Einstein relation)	$m^2 s^{-1}$
W_m	Metal work function	V
W_s	Semiconductor work function	V
χ	Electron affinity	V
$W_{ms} = W_m - W_s$	Metal-semiconductor work function difference	V
$\Delta\phi_{ms}$	Difference between metal work function and an intrinsic semiconductor reference $\Delta\phi_{ms} = W_{ms} - (E_f - E_i)/q = W_{ms} - U_T \ln(N_D/n_i)$	V
μ	Free-carrier mobility	$cm^2/V.s$
μ_n	Free electron mobility	$cm^2/V.s$
μ_p	Free hole mobility	$cm^2/V.s$
μ_0	Low-field surface mobility	$cm^2/V.s$
μ_{eff}	Effective carrier mobility	$cm^2/V.s$
U_T	Thermodynamic voltage	V
t_{ox}	Oxide thickness	m
X_{dep}	Depletion width	m
$C_{ox} = \epsilon_{ox}/t_{ox}$	Gate oxide capacitance	F/m^2
$C_{dep} = \epsilon_{si}/X_{dep}$	Depletion capacitance	F/m^2
C_{eq}	Series combination of C_{ox} and C_{dep}	F/m^2
N_D	Uniform donor concentration in channel	cm^{-3}
N_A	Uniform acceptor concentration in substrate	cm^{-3}
N_s	Trap density of states	cm^{-2}
n	Electron density	cm^{-3}
p	Hole density	cm^{-3}
T_{sc}	Silicon thickness	m
$T_{sc,min}$	Minimum silicon thickness in VeSFET	m
$T_{sc,max}$	Maximum silicon thickness in VeSFET	m
$C_{si} = \epsilon_{si}/T_{sc}$	Channel capacitance	F
W	Channel width	m
h	Channel height	m
Q_{fix}	Fixed-charge density	C/m^2
Q_m	Mobile charge density	C/m^2
$Q_{m,s}$	Local mobile charge density at source	C/m^2
$Q_{m,d}$	Local mobile charge density at drain	C/m^2
$Q_{m,FB}$	Local mobile charge density at flat band	C/m^2
$\overline{Q}_{m1,2}$	Internal mobile charge densities	C/m^2
$\overline{Q}_{m,s}$	Global source charge density	C/m^2
$\overline{Q}_{m,d}$	Global drain charge density	C/m^2
$Q_G = \overline{Q}_{m,s} + \overline{Q}_{m,d}$	Total gate charge density	C/m^2
$Q_{sc} = Q_m + Q_{fix}$	Total charge density in semiconductor	C/m^2
Q_{ss}	Interface charged trap density	C/m^2
$V_{GS,FB}$	Flat-band gate voltage at source	V
$V_{ch}(y)$	Channel potential	V
x	Coordinate across the gates	m
y	Coordinate along the channel	m

Symbol	Description	Unit
V_{GS}	Gate to source voltage	V
V_{DS}	Drain-to-source voltage	V
V_{th}	Threshold voltage	V
$\Psi(x)$	Potential distribution	V
$\Psi_s=\Psi(x=\pm \frac{T_{sc}}{2})$	Surface potential	V
$\Psi_0=\Psi(x=0)$	Center potential	V
E_s	Electric field at surface	V/m
I_{DS}	Drain current	A
V_{th}	Threshold voltage	V
V_T	Charge threshold voltage	V
R	Radius	m
θ	Mobility reduction coefficient	$1/V$
$\Psi_{0,FB}$	Center potential at flat-band	V
$\Psi_{s,FB}$	Surface potential at flat-band	V
Ψ_{BCP}	Body center potential	V
$\Psi_{BCP,min}$	Minimum body center potential	V
$\Psi_{s,min}$	Minimum surface potential	V
Ψ_{0c}	Critical value for the center potential	V
Ψ_{sc}	Critical value for the surface potential	V
Ψ_{ox}	Oxide potential	V
Ψ_{ext}	Extremum potential across two gates	V
X_{ext}	Extremum position across two gates	m
E	Electric field	V/m
E_s	Surface electric field	V/m
E_0	Center electric field	V/m
E_{ox}	Electric field in the oxide	V/m
E_x	Longitudinal electric field	V/m
E_y	Lateral electric field	V/m
E_t	Trap-energy level	eV
$V_{GS,crit}$	Critical value for the gate potential	V
$I_{critical}$	Critical value for the drain-to-source current	A
g_{ds}	Drain trans conductance	Ω^{-1}
g_m	Gate transconductance	Ω^{-1}
V_{bi}	Built-in potential	V
g_{ch}	Local channel conductance	Ω^{-1}
$S_{\Delta I_{DS}}$	PSD of drain current thermal noise	A^2/Hz
$S_{\Delta I_G}$	PSD of induced gate noise	A^2/Hz
$S_{\Delta I_{DS}\Delta I_{G^*}}$	PSD of cross-correlation noise	A^2/Hz
$C_{GD}=\partial Q_G/\partial V_{DS}$	Gate–drain intrinsic capacitance	F/m^2
$C_{GG}=\partial \underline{Q}_G/\partial V_{GS}$	Intrinsic gate capacitance	F/m^2
$C_{DD}=\partial \underline{Q}_{m,d}/\partial V_{DS}$	Drain–drain capacitance	F/m^2
$C_{SD}=\partial \underline{Q}_{m,s}/\partial V_{DS}$	Source–drain capacitance	F
$C_{DG}=\partial \underline{Q}_{m,d}/\partial V_{GS}$	Drain–gate capacitance	F/m^2
$C_{SG}=\partial \underline{Q}_{m,s}/\partial V_{GS}$	Source–gate capacitance	F
ω	Angular frequency	rad/s
f	Frequency	Hz